This is a repository copy of *Flow rate influence on sediment depth estimation in sewers using temperature sensors*.

White Rose Research Online URL for this paper:
https://eprints.whiterose.ac.uk/215576/

Version: Published Version

Article:

Regueiro-Picallo, M. orcid.org/0000-0002-4933-8550, Schellart, A. orcid.org/0000-0001-6494-8165, Jensen, H. orcid.org/0009-0006-1047-0622 et al. (3 more authors) (2024) Flow rate influence on sediment depth estimation in sewers using temperature sensors. Water Science & Technology, 89 (11). pp. 3133-3146. ISSN 0273-1223

https://doi.org/10.2166/wst.2024.193

Reuse
This article is distributed under the terms of the Creative Commons Attribution (CC BY) licence. This licence allows you to distribute, remix, tweak, and build upon the work, even commercially, as long as you credit the authors for the original work. More information and the full terms of the licence here: https://creativecommons.org/licenses/

Takedown
If you consider content in White Rose Research Online to be in breach of UK law, please notify us by emailing eprints@whiterose.ac.uk including the URL of the record and the reason for the withdrawal request.

eprints@whiterose.ac.uk
https://eprints.whiterose.ac.uk/

Water Science & Technology

© 2024 The Authors Water Science & Technology Vol 89 No 11, 3133 doi: 10.2166/wst.2024.193

Flow rate influence on sediment depth estimation in sewers using temperature sensors

Manuel Regueiro-Picallo [a,*], Alma Schellart [b], Henriette Jensen [b], Jeroen Langeveld [c], Maria Viklander [d] and Lian Lundy [d]

[a] Universidade da Coruña, Water and Environmental Engineering Group (GEAMA), Centro de Innovación Tecnolóxica en Edificación e Enxeñaría Civil (CITEEC), A Coruña, Spain
[b] The University of Sheffield, Sheffield, UK
[c] Delft University of Technology, Delft, The Netherlands
[d] Department of Civil, Environmental and Natural Resources Engineering, Luleå University of Technology, Luleå, Sweden
*Corresponding author. E-mail: manuel.regueiro1@udc.es

MR-P, 0000-0002-4933-8550; AS, 0000-0001-6494-8165; HJ, 0009-0006-1047-0622; JL, 0000-0002-0170-6721; MV, 0000-0003-0394-6128; LL, 0000-0003-1155-4132

ABSTRACT

Enhancing sediment accumulation monitoring techniques in sewers will enable a better understanding of the build-up processes to develop improved cleaning strategies. Thermal sensors provide a solution to sediment depth estimation by passively monitoring temperature fluctuations in the wastewater and sediment beds, which allows evaluation of the heat-transfer processes in sewer pipes. This study analyses the influence of the flow conditions on heat-transfer processes at the water–sediment interface during dry weather flow conditions. For this purpose, an experimental campaign was performed by establishing different flow, temperature patterns, and sediment depth conditions in an annular flume, which ensured steady flow and room-temperature conditions. Numerical simulations were also performed to assess the impact of flow conditions on the relationships between sediment depth and harmonic parameters derived from wastewater and sediment-bed temperature patterns. Results show that heat transfer between water and sediment occurred instantaneously for velocities greater than 0.1 m/s, and that sediment depth estimations using temperature-based systems were barely sensitive to velocities between 0.1 and 0.4 m/s. A depth estimation accuracy of ± 7 mm was achieved. This confirms the ability of using temperature sensors to monitor sediment build-up in sewers under dry weather conditions, without the need for flow monitoring.

Key words: annular flume, heat-transfer processes, sediment transport, temperature sensing, urban drainage systems

HIGHLIGHTS

- Combining temperature measurements and analysis of heat-transfer processes can be used to estimate sediment depths in sewers.
- Neglecting hydraulic variables barely affected the accuracy of the depth estimations.
- Temperature-based systems can be low-cost and easy to scale and implement in sewer systems.
- These devices can lead to optimal inspection and cleaning strategies, as well as in other urban drainage systems.

INTRODUCTION

Sediment build-up in sewer systems not only poses environmental concerns but also leads to significant operational costs associated with maintenance and cleaning. Sewer inspection and cleaning efforts are scarce in most countries, leading to loss of hydraulic capacity, blockages and, consequently, an increased risk of flooding in urban areas. These tasks are often carried out periodically based on past experiences, but without using observation-based criteria. This strategy may lead to high costs if maintenance is not required as regularly. Some countries, such as Austria, rely on periodic maintenance based on image observations (Plihal *et al.* 2014), although these solutions are difficult to scale due to their cost. Improved monitoring approaches for measuring sediment build-up in pipeline networks will enable more effective cleaning strategies and enhance the understanding of sediment transport dynamics. Measuring sediment build-up across an entire sewer system presents significant difficulties, such as accessibility and equipment limitations (Bertrand-Krajewski *et al.* 2021). Previous attempts to monitor sediment build-up consisted mostly of single-pipe measurements that required a high cost of supervision and maintenance (e.g., Lepot *et al.* 2017).

This is an Open Access article distributed under the terms of the Creative Commons Attribution Licence (CC BY 4.0), which permits copying, adaptation and redistribution, provided the original work is properly cited (http://creativecommons.org/licenses/by/4.0/).

Downloaded from http://iwaponline.com/wst/article-pdf/doi/10.2166/wst.2024.193/1436204/wst089113133.pdf
by guest

This research uses temperature measurements as a proxy for estimating sediment depths in sewer systems. Temperature acts as a natural non-conservative tracer, providing very useful information in many applications such as sewer flow measurements or combined sewer overflow detections (e.g., Dürrenmatt *et al.* 2013; Montserrat *et al.* 2015). Recent studies advanced towards the detailed understanding of heat-transfer dynamics on the pipe network scale, especially the fluid–headspace–soil interaction (Abdel-Aal *et al.* 2021; Figueroa *et al.* 2021). In parallel, Regueiro-Picallo *et al.* (2023, 2024a) demonstrated that heat-transfer processes in urban drainage systems can be used as a method for monitoring sediment depths using temperature sensors. The methodology consists of dual temperature measurements in the fluid and sediment-bed layers to measure sediment build-up through changes in temperature dynamics. This approach was inspired by similar techniques used in river streambeds, which effectively identified accumulation and erosion processes by analysing daily temperature patterns (DeWeese *et al.* 2017; Sebok *et al.* 2017).

Temperature-based sediment monitoring systems assume that flow conditions do not affect heat-transfer processes between the water and sediment layer and therefore no hydraulic variables need to be measured. However, wastewater flows in sewers introduce forced convection at the water–sediment interface. This study examines the influence of convective processes on the estimation of sediment depths using temperature-based systems that ignored hydraulic variables. For this purpose, laboratory experiments in an annular flume were performed using various sediment depths, water temperature gradients, and flow rates. The main advantages of this type of facility were the steady flow conditions and the room-temperature control system (Tait *et al.* 2003). In addition, a numerical analysis was carried out to examine the heat transfer at the sediment–water interface. Finally, conclusions and recommendations are made for the design and implementation of low-cost, low-power, and low-computational sensor-based solutions to improve the understanding of sediment build-up processes and maintenance strategies for urban drainage systems.

METHODS

Experimental equipment

The annular flume at the University of Sheffield (UK) was used to perform the experimental campaign (Figure 1 (left)). This facility was located in a temperature-controlled room, where the air temperature was set at 20 °C with a stability of ± 1 °C. The flume consisted of a rectangular cross-section 0.20 m wide and 0.48 m high. The side walls and the bottom plate were made of plexiglass and showed 2.20 m external and 1.80 m internal diameters. In addition, the flume included a top plate with a smooth PVC lid. The vertical position of the lid could be manually operated to match the desired water depth in the flume. Top (lid) and bottom (walls and base) plates could be rotated independently and in opposite directions to minimise

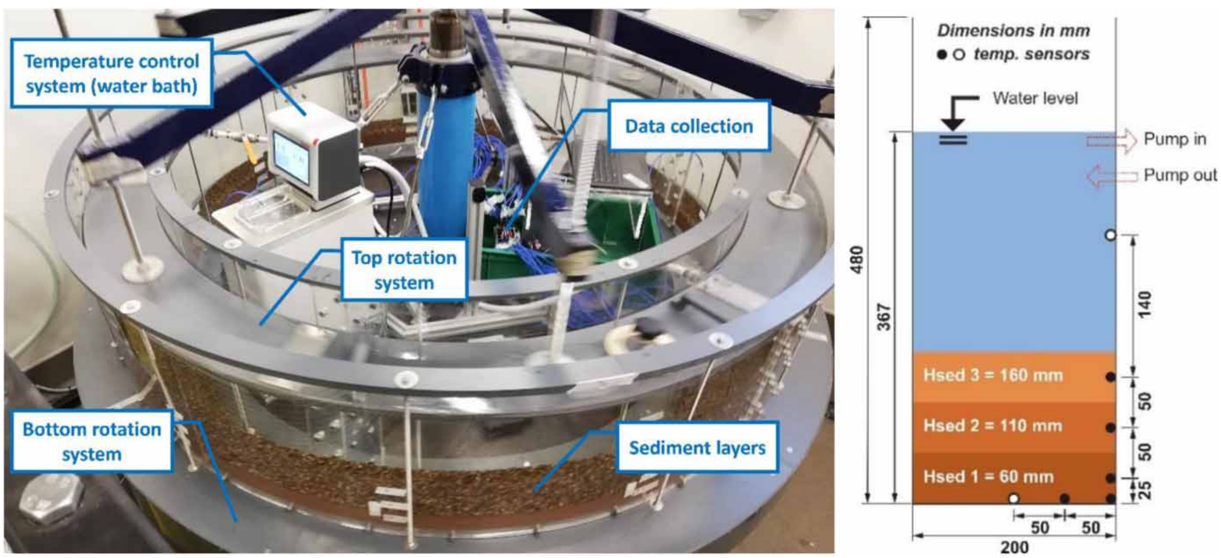

Figure 1 | Photo of the annular flume setup (left), and cross-section scheme of the temperature sensor installation (right). Temperature sensors symbolised with white dots were used to estimate the sediment depths (see Results section), while data related to black-dotted sensors are not shown in this study.

Downloaded from http://iwaponline.com/wst/article-pdf/doi/10.2166/wst.2024.193/1436204/wst089113133.pdf
by guest

the lateral flow circulations, establishing quasi-uniform shear stress conditions on the sediment bed (Tait *et al.* 2003; Cecchetto 2017). The rotational velocities of the top and bottom plates were controlled using an automatic control system.

The flume was equipped with 24 PT100 temperature sensors (RS Pro, UK) distributed in three cross-sections, covering the temperature measurements of the room, water, and sediment layer (see example in Figure 1 (right)). The data were controlled and collected in a laptop using temperature input modules at a frequency of 1 Hz (National Instruments – NI, UK). In addition, a water bath circulator (Julabo, UK) was installed on the bottom plate to simulate wastewater temperatures in sewers. To this end, a closed loop system was designed by connecting inlet and outlet hoses between the water bath and the annular flume.

The sediment bed consisted of a main layer of fine silica sand and a 10-mm top layer of coarse sand and gravel to avoid resuspension of fines and ensure a constant sediment depth during the experiments (no bed forms). The sediments were saturated before layering in the flume to prevent air voids. Furthermore, sub-samples were taken and analysed according to standardised methods to characterise the physical and thermal properties. Densities were determined from laboratory analysis while thermal properties (thermal conductivity and volumetric heat capacity) were measured by using a TP01 sensor (Hukseflux, The Netherlands).

Procedure

The laboratory-scale experiments replicated water temperature fluctuations in sewer pipes during dry weather periods. These fluctuations show marked daily, cyclical patterns which can be characterised by a phase and an amplitude (Regueiro-Picallo *et al.* 2023). Experiments were carried out by establishing daily temperature patterns using the water bath circulator and flow conditions by setting top–bottom rotational velocities. In addition, the flume was filled with sediment layers, establishing three sediment depth conditions (H_{sed}: 60, 110, and 160 mm), and a layer of tap water was added on top. The objective was to measure the temperature time series in the system (water and sediment layers) and estimate the sediment depth by analysing the heat-transfer process.

The water bath circulator was programmed to simulate wastewater temperatures in sewers during dry weather periods, when sediment build-up is likely to occur. In-sewer measurements from the Urban Water Observatory (UWO), which is operated by the aquatic research centre Eawag (Dübendorf, Switzerland) in the municipality of Fehraltorf (Switzerland), were used as a reference (Blumensaat *et al.* 2023). Two temperature patterns were established in the water layer with daily temperature gradients (ΔT) of 3.0 and 5.5 °C to test the sensitivity of the temperature amplitude in heat transfer to the sediment layer (Figure 2), where the temperature gradients were defined as the difference between daily maximum and minimum temperatures. The temperature patterns were tested for two daily cycles (48 h), trying to minimise the influence of the initial conditions.

An optimal ratio between top and bottom rotational velocities was used to establish the flow conditions while minimising the effect of lateral flow circulations (Cecchetto 2017). This ratio is influenced by the flume geometry (radius, width, and wall roughness), the water depth and viscosity, and the sediment roughness. Flume dimensions, water viscosity, and sediment roughness were assumed to be constant, while the water depth depended on the height of the water surface (constant) and the sediment depth. Therefore, a calibration of the optimal ratio was performed for each sediment depth condition.

Near-neutral buoyancy balls were introduced in the annular flume to perform the optimal rotational ratio calibration. The rotational velocities, ω (rad/s), were measured by timing a set of plate rotations to obtain the time per lap, t (s), and expressed as $\omega = 2\pi/t$. After establishing a bottom rotational velocity (ω_b), the top rotational velocity (ω_t) was visually adjusted to a value at which the ball was rolling at the centre of the cross-section. This process was performed by two observers to avoid bias and repeated up to nine steps, ranging bottom rotational velocities from 0.25 to 0.45 rad/s to avoid null ball movement for low velocities and sediment bed erosion for high velocities (Figure 3). Finally, the average optimal ratio, ω_{opt}, was considered to establish the flow conditions, resulting in values of $\omega_{opt} = 3.84$, 3.74, and 3.38 for sediment depths of 60, 110, and 160 mm, respectively (e.g., Cecchetto 2017).

Three flow velocities, expressed as a function of the rotational velocity and the mean radius of the flume ($R = 1$ m), $u = \omega R$, were tested in the annular flume. The bottom velocity, u_b (m/s), was used as the characteristic velocity of the annular flume to set flow conditions of 0.1, 0.2, and 0.4 m/s (Booij 1994). Subsequently, top velocities, u_t (m/s) were determined and set by applying the optimal ratio. In summary, 18 experiments were performed, combining three sediment depths (H_{sed}: 60, 110, and 160 mm), two temperature patterns (ΔT: 3.0 and 5.5 °C) and three flow conditions (u_b: 0.1, 0.2, and 0.4 m/s).

Downloaded from http://iwaponline.com/wst/article-pdf/doi/10.2166/wst.2024.193/1436204/wst089113133.pdf
by guest

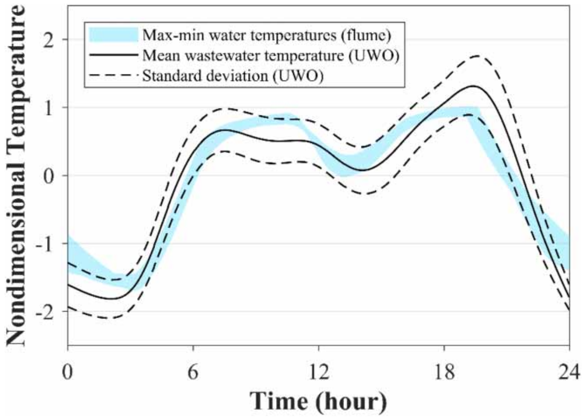

Figure 2 | 24-h comparison between the water temperature time series in the experimental campaign and the wastewater temperatures measured at the UWO. Note that non-dimensional temperatures (U) were plotted, which were computed as $U = (T - \bar{T})/A$, where T and $\bar{T}$ are the instantaneous and mean temperatures (°C), respectively, and (A) is the amplitude (°C).

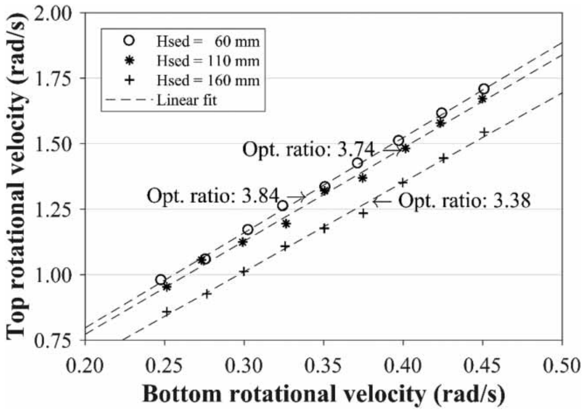

Figure 3 | Optimal rotational ratio calibration for the sediment depths of 60 mm (o), 110 mm (*), and 160 mm (+). Dashed lines represent the linear regression between the top and bottom rotational velocities.

Heat-transfer models to perform sediment depth estimations

Temperature daily patterns in combined sewer pipes depend on basin activities, habits, and network operation strategies, but also heat-transfer processes, such as sewer ventilation, and the characteristics of the pipes and the surrounding soil (Figueroa *et al.* 2021). Wastewater temperatures in combined sewer systems show substantial fluctuations, which guarantee the required dynamics to detect sediment build-up (Regueiro-Picallo *et al.* 2023). As for hydrodynamics, these systems operate most of the time under dry weather flow (DWF) conditions. Sediment build-up can result from low flow velocities and high concentrations of suspended particles, leading to reduced hydraulic capacity in sewer systems. The sediment layer introduces additional heat-transfer processes at the wastewater–pipe–soil system, as shown in Figure 4. Particularly, heat transfer in the sediment layer is governed by diffusion processes.

The methodology for estimating sediment depths in sewers using temperature measurements and heat-transfer analysis is based on the installation of sensors on the perimeter of pipes to detect changes in the cyclic temperature patterns (Regueiro-Picallo *et al.* 2023), as well as the consideration of sediment thermal properties and heat loss at the bottom boundary (i.e., sediment–pipe–soil system). The greater the change in temperature patterns between a sensor in the wastewater layer and one in the sediment layer, the greater the sediment depth. Conversely, no sediment deposits are assumed if the temperature time series are nearly constant at the wetted perimeter. The amplitude (A, °C) and phase (ϕ, rad) decomposition of the sinusoidal signal was used to establish features to relate the sediment depths (Tonina *et al.* 2014). As temperatures show a daily

Downloaded from http://iwaponline.com/wst/article-pdf/doi/10.2166/wst.2024.193/1436204/wst089113133.pdf
by guest

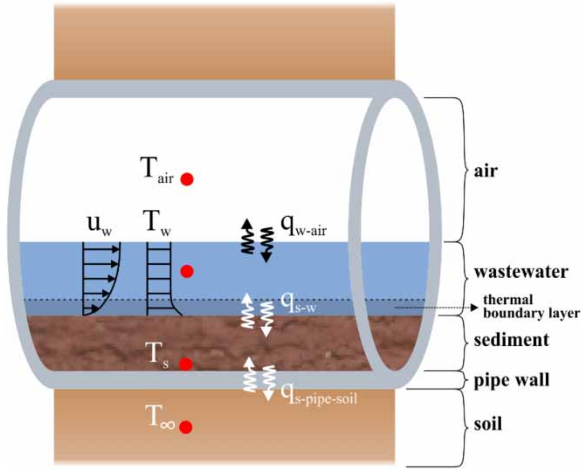

Figure 4 | Distribution of heat transfer processes between water (w-subscript), sediment (s-subscript), pipe, and soil in a sewer pipe.

pattern, the fundamental frequency (or first harmonic) of the temperature series in the water and sediment layers was evaluated, establishing the following features:

$$A_{\mathrm{r}} = \frac{A_{\mathrm{s}}}{A_{\mathrm{w}}} \tag{1}$$

$$\Delta\phi = \phi_{\mathrm{s}} - \phi_{\mathrm{w}} \tag{2}$$

where A_{r} is the amplitude ratio and $\Delta\phi$ is the phase difference (rad) between the temperature time series in the water and sediment layers. In addition, s and w are the subscripts relative to the sediment and water layers, respectively. The fast Fourier transform (FFT) algorithm was used to evaluate signal decomposition.

Regueiro-Picallo *et al.* (2024a) presented a simplified surrogate model to estimate sediment depths in sewer pipes based on the comparison of the water and sediment-bed temperature time series (i.e., A_{r} and $\Delta\phi$), the sediment thermal properties and the pipe wall heat loss. The surrogate model was developed based on the solution of the 1D heat diffusion equation in the sediment bed (domain), establishing a Cauchy-type (or mixed) bottom boundary condition that reproduces the heat loss of the sediment–pipe–soil system, and a Dirichlet-type top boundary condition that assumes instantaneous heat transfer between the water and the sediment layer. The equations describing the 1D heat diffusion model in the sediment layer are shown in the following:

$$\frac{\partial T}{\partial t} = k_{\mathrm{e}} \frac{\partial^2 T}{\partial z^2} \tag{3}$$

where T is the temperature (°C), t is the time (s), z is the vertical dimension (m), and k_{e} denotes the effective thermal diffusivity of the sediment layer (m^2/s) that represents the ratio of the thermal conductivity (k_{t}, W/m/°C) and the volumetric heat capacity (C_{v}, $\mathrm{J/m^3/°C}$), $k_{\mathrm{e}} = k_{\mathrm{t}}/C_{\mathrm{v}}$.

$$-k_t \frac{dT}{dz}\bigg|_{\Delta z} = h(T_{\Delta z} - T_{\infty}) \tag{4}$$

where Δz is the relative vertical position of the sediment bottom (m) that depends on the sediment depth (H_{sed}, m), h is the convective heat-transfer coefficient at the bottom boundary ($\mathrm{W/m^2/°C}$) that depends on the material (e.g., PVC or concrete in sewer pipes) and its thickness, $T_{\Delta z}$ is the sediment temperature at the bottom (°C), and T_{∞} is the temperature outside the domain (°C).

$$T_w = f(t) \tag{5}$$

Downloaded from http://iwaponline.com/wst/article-pdf/doi/10.2166/wst.2024.193/1436204/wst089113133.pdf
by guest

where T_w is the temperature of the water layer (°C). Equation (3) represents the 1D heat diffusion equation in the sediment layer, and Equations (4) and (5) simulate the bottom and top boundary conditions, respectively.

Water motion over the sediment surface enhances heat transfer, i.e., the higher the flow velocity, the greater the heat-transfer rate. Instantaneous heat transfer between water and sediment layers can be assumed if the flow velocity is very large. However, heat-transfer processes at the water–sediment interface can be influenced by low flow velocity conditions, i.e., sediment build-up conditions. A Cauchy-type condition can strictly reproduce the forced convection heat transfer at the water-sediment interface due to the flow conditions, similar to the bottom boundary condition (Equation (4)). Therefore, the top boundary condition of the 1D heat diffusion model can be modified to evaluate the influence of the flow conditions:

$$-k_t \frac{dT}{dz}\bigg|_{z_0} = h_w (T_{z_0} - T_w) \tag{6}$$

where z_0 is the relative vertical position of the water–sediment interface (m), T_{z0} is the sediment temperature at the top boundary (°C), and h_w is the convective heat-transfer coefficient at the top boundary (W/m^2/°C) that can be expressed as follows for a flat surface (Hewitt *et al.* 1994), e.g., sediment bed:

$$h_w = \frac{Nu_L k_{t_w}}{L} \tag{7}$$

where L is the characteristic length of the flat surface (m), i.e., flume length ($L = 6.28$ m), k_{t_w} is the thermal conductivity of the water, assumed to be $k_{t_w} = 0.598$ W/m/°C, and Nu_L is the Nusselt number that represents the non-dimensional heat-transfer coefficient in flat surfaces and relates the Reynolds (Re_L) and Prandtl (Pr) numbers. The averaged Nusselt number over an isothermal plate in a turbulent region can be expressed as follows:

$$Nu_L = 0.037 Re_L^{4/5} Pr^{1/3} \; 0.6 \le Pr \le 60 \text{ and } 5 \times 10^5 \le Re_L \le 10^7 \tag{8}$$

where Re_L is the Reynolds number expressed as $Re_L = uL/\nu$, where u is the flow velocity (m/s) and ν is the kinematic viscosity of the water (m^2/s) assumed to be $\nu = 10^{-6}$ m^2/s, and Pr is the Prandtl number expressed as $Pr = \nu \rho_w c_{p_w} / k_{t_w}$, where ρ_w and c_{p_w} are the density (kg/m^3) and the specific heat capacity (J/kg/°C) of the water, respectively ($\rho_w = 997$ kg/m^3 and $c_{p_w} = 4186$ J/kg/$^\circ$C), resulting in $Pr = 7.0$.

In summary, two models differentiated by the top boundary condition (Dirichlet and Cauchy) were defined to evaluate the influence of flow velocity on heat-transfer processes in the water-sediment boundary and, consequently, on the sediment depth estimations. For this purpose, a numerical analysis was performed to compare both models by simulating the temperatures in the sediment layer under multiple flow velocity and sediment depth conditions. Moreover, experimental temperature measurements at the bottom of the sediment layer were compared with water temperatures to calculate harmonic characteristics and, subsequently, to estimate sediment depths in the experiments by applying the simplified surrogate model. The estimations were compared with reference depth measurements to evaluate the uncertainty of ignoring flow conditions in the surrogate model.

RESULTS

Effective sediment properties

The physical and thermal properties of the sediments, i.e., fine and coarse sands, and gravels, were determined from laboratory analysis and sensor-based measurements, considering a composite sub-sample to analyse the thermal properties of coarse sands and gravels (Table 1). The effective thermal properties were calculated to describe the heat-transfer characteristics of a multi-layer system since the sediment bed consisted of various materials. The series model with horizontal layer distribution was used to calculate the effective thermal conductivity, $k_t = H_{sed}/(H_{sedf}/k_{tf} + H_{sedc}/k_{tc})$, where f and c are the subscripts relative to the fine sand layer and to the composite layer of coarse sand and gravel, respectively (Radhakrishnan *et al.* 2010). Moreover, the volumetric heat capacity of a two-layer system was determined by the formula $C_v = (H_{sedf}/H_{sed})C_{vf} + (H_{sedc}/H_{sed})C_{vc}$ (Marín *et al.* 1996). As a result, a value of effective thermal conductivity and volumetric heat capacity was obtained for each sediment depth condition. Average effective thermal properties were assumed

Downloaded from http://iwaponline.com/wst/article-pdf/doi/10.2166/wst.2024.193/1436204/wst089113133.pdf
by guest

Table 1 | Physical and thermal properties of the sediments: dry bulk density (kg/m^3), thermal conductivity (W/m/°C), and volumetric heat capacity (MJ/m^3/°C)

Sample	Dry density (kg/m^3)[a]	Thermal conductivity (W/m/°C)[b]	Volumetric heat capacity (MJ/m^3/°C)[b]
Fine sand	1,440–1,790	1.88–1.92	2.52–2.67
Coarse sand	1,480–1,750	1.95–1.99[c]	2.85–3.00[c]
Gravel	1,490–1,730		
Reference values (sand)	1,400–2,000[d]	1.16–2.18[d]	2.40–3.04[e]
Effective thermal properties (mean values)	1.91	2.62	

Minimum and maximum values.
[a]Laboratory analysis.
[b]Sensor-based measurements.
[c]Composite sample.
[d]Nikiforova *et al.* (2013).
[e]Abu-Hamdeh (2003).

for the later heat-transfer analysis and sediment depth estimation, as the maximum relative deviations were less than 1% for both thermal conductivity and volumetric heat capacity. Measured sediment properties were similar to reference values for submerged and saturated sands (Abu-Hamdeh 2003; Nikiforova *et al.* 2013), and to sewer sediments with low organic matter content (Regueiro-Picallo *et al.* 2024a).

Fluctuations of water temperature in the sediment bed at different depths

The sediment bed temperature series were damped and time-shifted compared to the water temperature. The greater the sediment depth, the greater the amplitude attenuation and phase shift between the water and sediment-bed temperature series (Figure 5). The harmonic features, i.e., amplitude ratio (A_r) and the phase difference ($\Delta\phi$), were computed to quantify the attenuation and phase shift between the temperature series. These values were calculated using the 48-h time series and expressed as ranges covering the three flow conditions and the two temperature patterns for each sediment depth. Thus, A_r-values ranged [0.90, 0.93], [0.73, 0.75], and [0.52, 0.60] for depths of 60, 110, and 160 mm, respectively. Similarly for the phase shift, $\Delta\phi$-values ranged [0.16, 0.19], [0.46, 0.50], and [0.78, 0.84] for depths of 60, 110, and 160 mm, respectively. The main differences between the harmonic features were related to depth and, less significantly, to velocity conditions and temperature patterns.

The water temperature fluctuations in the sediment layer were also numerically simulated with the two 1D heat diffusion models, i.e., with Dirichlet- and Cauchy-type top boundary conditions. In addition to the water temperature time series, the sediment thermal properties (k_t and C_v), the convective heat-transfer coefficient at the bottom boundary (h), the temperature outside the model (T_∞), and the initial temperature of the sediment bottom (T_{s0}) were considered to simulate the temperatures at the bottom of the sediment layer. Moreover, the diffusion model with the Cauchy-type top boundary condition also considered the hydraulic conditions (u_b and L). Most of the above variables were measured (temperature, flow velocity, and flume geometry) or characterised by laboratory analysis (sediment thermal properties). The convective heat-transfer coefficient at the bottom boundary (h) was calibrated by fitting the experimental data and the simulated sediment temperatures using the heat diffusion models for large flow conditions, i.e., $u_b = 0.4$ m/s, as large velocities barely influence the heat-transfer process at the water–sediment interface. The result of the calibration process was $h = 2.6$ W/m^2/°C. In addition, the mean room temperature was considered as the temperature outside the domain (T_∞), which represents the soil temperature under actual conditions. Finally, the initial temperature of the sediment bottom (T_{s0}) was established by performing a 24-h warmup period of the model.

The Nash–Sutcliffe model efficiency coefficient (NSE) was used to compare the performance of the numerical models to simulate the sediment temperatures, taking the temperature measurements at the sediment bottom as reference observations (Figure 5). The NSE values ranged from 0.83 to 0.99 for the diffusion model with the Dirichlet-type top boundary condition, while for the model with the Cauchy-type top boundary condition, the NSE values ranged from 0.82 to 0.99. A strong fit between experimental and numerical temperatures was obtained (median NSE values were 0.98), which means that both models accurately reproduced the heat-transfer process in the sediment layer. No major differences between the NSE values were found and, consequently, both models can yield similar sediment depth estimations. The following section

Downloaded from http://iwaponline.com/wst/article-pdf/doi/10.2166/wst.2024.193/1436204/wst089113133.pdf
by guest

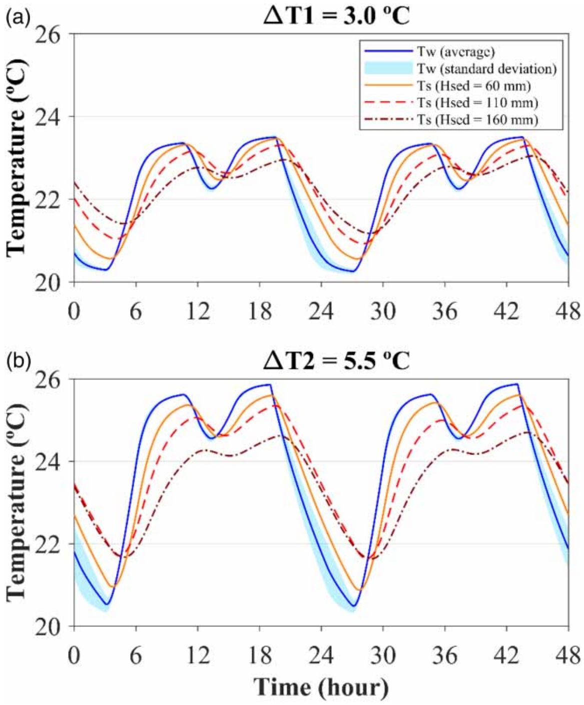

Figure 5 | Temperature time series in the water layer (mean: blue line, standard deviation: blue filled area) and sediment bottom (H_{sed}: 60, 110, and 160 mm) for temperature patterns $\Delta T1$ (a) and $\Delta T2$ (b). Mean and standard deviation of temperature time series were calculated using the measurements from the three monitored sections.

presents a numerical comparison between the 1D heat diffusion models to analyse the influence of the flow conditions on the top boundary of the sediment layer.

Sensitivity of flow conditions on heat transfer between water and sediment layer

A fluid flowing over a surface generates a thermal boundary layer, which induces a convection process. In the present study, the wastewater flowing over the sediment bed induced a forced convection between both layers. The heat-transfer process at the sediment–water interface can be characterised by the convective heat-transfer coefficient, h_w (Equation (7)), which is related to the Nusselt number, Nu_L. High h_w values indicate small thicknesses of the thermal boundary layer and, consequently, equal temperatures in the water layer and water-sediment contour. h_w is expressed as a function of Reynolds and Prandtl numbers (Equation (8)), which relate inertial (hydraulic), thermal, and viscosity variables. Assuming that the water thermal properties and viscosity were constant in the experimental campaign, the convective heat-transfer coefficient between the water and sediment layers was only sensitive to the Reynolds number. Furthermore, h_w can be assumed to be more sensitive to the flow velocity than to the characteristic length since the proportion to the latter is $h_w \propto L^{1/5}$.

Temperatures at the bottom of the sediment layer were simulated with 1D heat-transfer models including Dirichlet- and Cauchy-type top boundary conditions to study the influence of flow conditions on heat-transfer processes and, consequently, on the sediment depth estimation. The simulated sediment temperatures were calculated using the following simplified input variables: (i) the mean water temperature time series of the experiments with a daily gradient of 5.5 °C; (ii) the effective thermal properties of the sediments; (iii) the heat loss condition at the bottom boundary, defined by $h = 2.6\ \mathrm{W/m^2/°C}$; and (iv) a range of sediment depths between 10 and 190 mm. Moreover, the flume length ($L = 6.28$ m) was selected as the characteristic length, and Reynolds numbers ranging from 5×10^5 to 5×10^6, which were equivalent to bottom velocities of $u_b = [0.1, 0.8]$ m/s, were also considered for the simulations with the model that included the Cauchy-type top boundary condition.

The harmonic features between the time series of water temperature and the simulated temperatures at the bottom of the sediment layer were calculated for each sediment depth (Figure 6). The higher the Reynolds number, the stronger the

Downloaded from http://iwaponline.com/wst/article-pdf/doi/10.2166/wst.2024.193/1436204/wst089113133.pdf
by guest

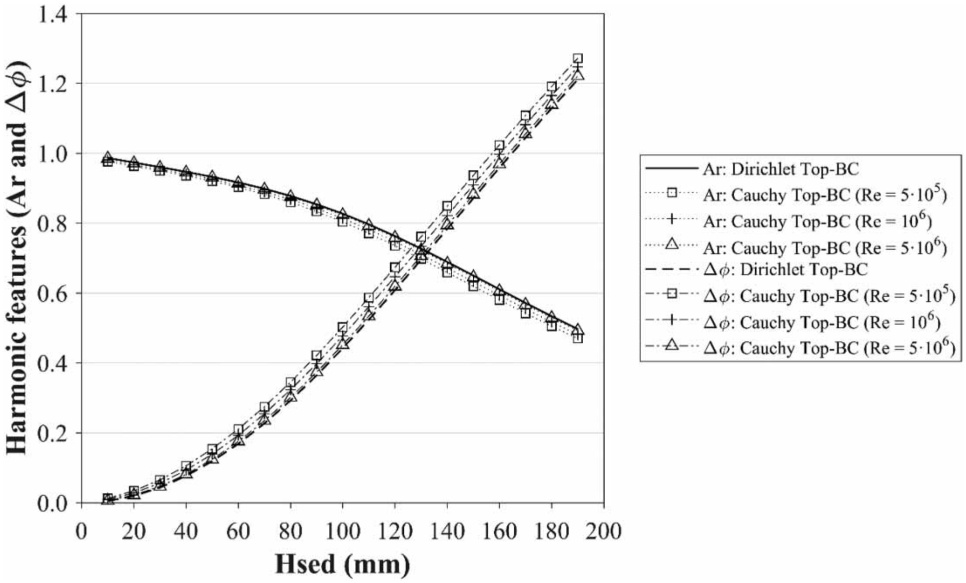

Figure 6 | Relationships between harmonic features and sediment depths. Amplitude ratio and phase differences were calculated from water and sediment temperatures, which were simulated with the 1D heat diffusion models including Dirichlet- and Cauchy-type top boundary conditions.

agreement between the results of the models with Dirichlet- and Cauchy-type top boundary conditions. The differences between the two models were negligible by taking the convective heat-transfer coefficient between the water and sediment layer as a reference because the h_w-values were very large ($h_w \geq 244$ W/m^2/°C) compared, for example, with the convective heat-transfer coefficient at the bottom of the sediment layer ($h = 2.6$ W/m^2/°C). Therefore, a Dirichlet-type boundary condition can be assumed to simulate heat-transfer processes at the water–sediment interface ($T_{z0} = T_w$) under low flow conditions in sewers and, consequently, to estimate the sediment depth applying the surrogate model (Regueiro-Picallo *et al.* 2024b).

Sediment depth estimations

Harmonic features were used as input of the surrogate model to estimate the sediment depths. The FFT algorithm was applied at 24-h moving intervals to calculate the uncertainty of the harmonic features and, consequently, of the depth estimations. The remaining inputs were (i) the average room temperature, which simulated the soil temperatures; (ii) the mean effective sediment thermal properties (Table 1); and (iii) the convective heat-transfer coefficient of the bottom boundary, which was constant and depended on the material at the bottom of the flume. Note that no input parameters related to the flow were required to perform the sediment depth estimations with the surrogate model. Small deviations were observed between the sediment depth estimations obtained with the temperature-based system and the reference depth measurements (Figure 7). The overall accuracy of the temperature-based system estimations was ± 7 mm, similar to previous work without flow conditions (Regueiro-Picallo *et al.* 2024a).

The uncertainty of the sediment depth estimations for small temperature gradients ($\Delta T = 3.0$ °C) was greater than for large gradients ($\Delta T = 5.5$ °C). Consequently, the larger the daily temperature gradient the more precise estimations could be obtained. Moreover, the estimation uncertainty was not affected by the sediment depth, i.e., the precision was similar for the range of sediment depths tested (60, 110, and 160 mm). However, the precision will decrease for larger depths ($h_{sed} \geq 160$ mm) because the attenuation and time-shift of the temperature time series at the sediment bottom will be very large, particularly for organic sediments with low thermal diffusivities (Regueiro-Picallo *et al.* 2023). Furthermore, the sediment depth estimations generally decreased as the flow increased because of the convective heat-transfer process in the water-sediment interface (Figure 6). However, the deviations between the depth estimations considering the flow conditions did not exceed 10 mm, showing that the flow rate and, subsequently, the convective term had minimal impact on sediment depth estimations.

Downloaded from http://iwaponline.com/wst/article-pdf/doi/10.2166/wst.2024.193/1436204/wst089113133.pdf
by guest

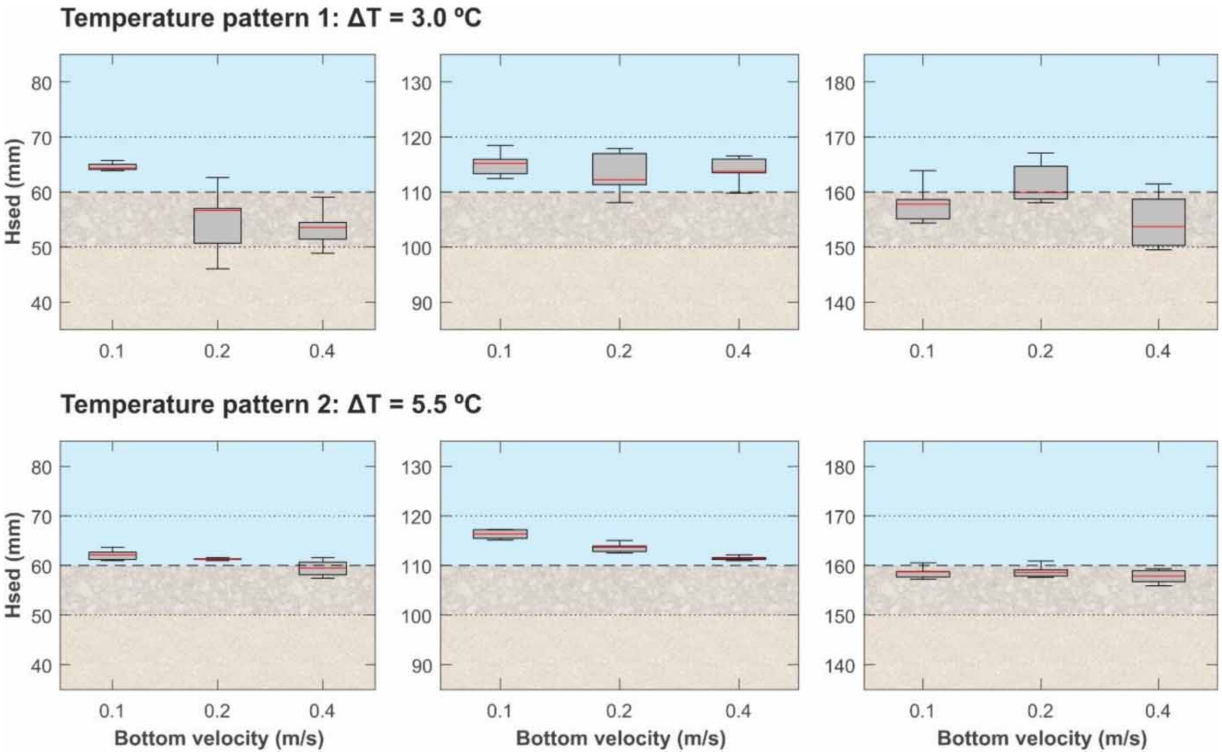

Figure 7 | Comparison of the sediment depths estimated with the temperature-based system (boxplots) and the reference measurements (dashed lines) at 60- (left plots), 110- (middle plots), and 160-mm (right plots), considering three bottom velocities (0.1, 0.2, and 0.4 m/s) and two temperature patterns ($\Delta T = 3.0$ °C: top plots, and $\Delta T = 5.5$ °C: bottom plots). Dotted lines symbolise a ± 10 mm bound.

DISCUSSION

The performance of temperature-based systems for estimating sediment depths in sewers was evaluated considering different flow conditions and temperature daily patterns. Low flow velocities, $u_b = 0.1$, 0.2, and 0.4 m/s, which are likely to sediment accumulation (Lange & Wichern 2013; Regueiro-Picallo *et al.* 2017), were tested. The bottom plate velocity was taken as a reference to establish the flow conditions as it is the characteristic velocity in annular flumes (Booij 1994). The results showed that the convective heat-transfer processes at the water–sediment interface due to the flow velocity could be neglected because they barely influenced the sediment depth estimation. Minimal deviations of the sediment depth estimations were obtained using the surrogate model, which excludes the convective heat-transfer coefficient in the top boundary (h_w). h_w-values were very large for flow velocities higher than 0.1 m/s and therefore instantaneous heat transfer between the water and sediment layers can be assumed. Consequently, temperature-based systems can be used to monitor sediment accumulation in sewer systems without requiring the measurement of hydraulic variables, e.g., flow rates or water depths. Nevertheless, other variables, such as the sediment thermal properties and the convective heat-transfer coefficient at the sediment bottom, must also be considered to estimate sediment depths accurately.

Temperature fluctuations in urban drainage systems can be measured using the MONitoring Temperatures in SEdiments (MONTSE) device (Regueiro-Picallo *et al.* 2024a). MONTSE is comparable to distributed temperature sensing (DTS) devices, which are commonly deployed to detect illicit connections as well as infiltration and inflow into sewers (e.g., Vosse *et al.* 2013; Panasiuk *et al.* 2019). The vertical resolution of sensors of MONTSE permits the monitoring of temperature fluctuations by comparing measurements from sensors exposed to air, submerged in water, and buried in sediments. In addition, MONTSE includes a Dual-Probe Heat-Pulse (DPHP) module for *in situ* determination of sediment thermal properties, which consists of a heater cartridge that induces a heat pulse while a temperature sensor measures the response across the sediment bed (e.g., Ravazzani 2017; He *et al.* 2018). DPHP measurements are local, and, unlike sands and gravels, the thermal properties of organic sediments can oscillate both spatially and temporally due to biological processes, similar to the physicochemical properties of sewer sediments (Ristenpart 1995; Regueiro-Picallo *et al.* 2020). Small uncertainties can

Downloaded from http://iwaponline.com/wst/article-pdf/doi/10.2166/wst.2024.193/1436204/wst089113133.pdf
by guest

be assumed when using local measurements of thermal properties to estimate sediment depth (Regueiro-Picallo *et al.* 2024a). Furthermore, the convective heat transfer coefficient at the sediment bottom depends on the composition and thickness of the material in contact with the sediments (e.g., pipe), and can be assumed to be constant. The coefficient can be estimated with prior knowledge of the sewer system, although it is also possible to calibrate from reference sediment depth measurements, as for the experimental campaign.

The sediment depth estimations were computed using a simplified surrogate model, which was mainly based on the relationship with the harmonic characteristics of the water and sediment temperature time series as well as the sediment thermal properties and the convective heat-transfer coefficient at the sediment–pipe–soil boundary. A decomposition of the temperature fluctuations was performed to calculate the harmonic features (FFT algorithm). The annular flume was operated for a minimum period of 24 h prior to the start of each experiment with the aim of establishing the initial temperature conditions in the sediment layer and, consequently, minimise the oscillation of the harmonic features. Only the fundamental frequency (or first harmonic) was later considered as input to the surrogated model, although, as the time series shows two peaks during the day, the second harmonic could be added to the model to improve the depth estimations.

The surrogate model was based on the solution of the 1D heat diffusion equation at the bottom of the sediment layer. Despite the installation of a temperature sensor at the centre of the flume base ($B/2 = 100$ mm), the heat-transfer processes exhibited a dependence on the lateral contours. The influence of the flume walls was evaluated by comparing simulated temperatures at the bottom of the sediment layer using 1D and 2D heat diffusion models (Figure 8). The median absolute deviation (MAD) was used to compare the 1D and 2D simulated temperatures, yielding the maximum deviations for the smallest ratios between the flume width (B) and the sediment depth, B/H_{sed}. Deviations were less than 0.15 °C for those experimental conditions with $H_{sed} = 160$ mm and water temperature gradients of 5.5 °C, which represents a relative error of less than 3%.

The 2D heat diffusion model of the sediment layer can be applied as an alternative method for estimating sediment depths, for example, by identifying the best fit between the simulated temperatures and the sensor measurements on the flume walls (Figure 1(b)). In the event of large sediment depths and significant convective heat transfer through the sediment–pipe–soil boundary, temperature fluctuations at the bottom of the sediment layer will be significantly attenuated in relation to water temperatures, leading to highly uncertain depth estimations. Under these conditions, the vertical sensor distribution on the wall will enable the identification of sensors buried in the sediment layer, as well as the estimation of the position of the sediment–water interface and, consequently, the sediment depth (e.g., Sebok *et al.* 2017). Only measurements from sensors located in the water layer and at the bottom of the sediment layer (centre of the flume base) were considered in this study because the temperature fluctuations at the bottom of the sediment layer were not fully attenuated for the worst conditions, $H_{sed} = 160$ mm, resulting in accurate depth estimations (± 7 mm). The sediment depth estimation range can be approached using the diurnal damping depth (Luce *et al.* 2013), expressed as $z_d = \sqrt{2k_e/\omega}$, where ω is the fundamental frequency (s^{-1}), or $\omega = 2\pi/P$, where P is the period of the daily fluctuations (s), equal to 86,400 s. The diurnal damping depth relates time-, distance-scales and sediment thermal properties, and expresses the depth at which the amplitude of daily temperature fluctuations is $1/e$ of that at the surface, i.e., water-sediment boundary. A value of $z_d = 142$ mm was obtained for the type

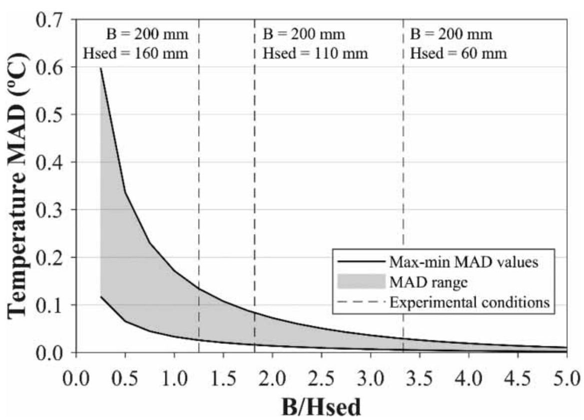

Figure 8 | Deviations of simulated temperatures at the bottom of the sediment layer using the 1D and 2D heat diffusion models as a function of the flume width and the sediment depth conditions.

Downloaded from http://iwaponline.com/wst/article-pdf/doi/10.2166/wst.2024.193/1436204/wst089113133.pdf
by guest

of sediments that were tested in the experimental campaign. Organic sediments, such as sewer sediments, can show lower k_e-values than sands and gravels and, consequently, lower sediment depth estimation ranges.

In concluding remarks, temperature-based systems could be low-cost and easy to scale and implement in sewer systems, leading to optimal inspection and cleaning strategies based on observations rather than periodic operations. This would reduce costs and the risk of combined sewer overflows (CSO) during rainfall events caused by sediment accumulation. Monitoring sediment build-up could also be used to develop accurate sediment transport models in sewer systems, resulting in optimal sewer system designs and the development of digital twin models. Future commercial and scientific perspectives include the installation of these systems to optimise the sediment management in sewer systems and other urban drainage infrastructures, such as sediment collectors.

CONCLUSIONS

Heat-transfer processes in sewers were investigated while considering the presence of sediment accumulation. The sediment layer provides a dampening effect on the temperature fluctuations of the wastewater, which follow a cyclical pattern under dry weather conditions. Temperature damping can be expressed by means of harmonic characteristics and is mainly affected by the sediment depth, as well as the sediment thermal properties, the heat loss at the boundaries and the flow velocity.

An experimental campaign was performed in an annular flume by reproducing heat-transfer processes in combined sewer systems under DWF conditions. This allows for the evaluation of the influence of hydraulic conditions and temperature patterns when estimating sediment depth using temperature-based systems. A numerical analysis of heat transfer models was carried out considering the influence of flow-forced convection at the water-sediment interface. Large values of the convective heat-transfer coefficient at the water–sediment interface were obtained, indicating that the temperature boundary layer above the interface was very small and, consequently, heat transfer occurred instantaneously for velocities greater than 0.1 m/s. Therefore, the hydraulic conditions in sewers hardly influenced the heat-transfer processes of sediment bed deposits. This allowed the use of simplified surrogate models based on the comparison of water and sediment-bed temperature measurements to estimate sediment depths, i.e., ignoring hydraulic variables.

Sediment depth estimations showed a low uncertainty and a high precision compared to the reference depth measurements when there was a large daily amplitude. In addition, deviations of the depth estimates were less than 10 mm considering the different flow velocity conditions established in the flume. These results confirmed that systems based on temperature measurements are a viable solution for sediment monitoring in combined sewer pipes without measuring hydraulic variables. Moreover, sediment thermal properties and convective heat transfer at the sediment–pipe–soil boundary must be determined. Effective thermal properties of the sediment were characterised in the experimental campaign using sub-samples, although heat-pulse methods can also be applied for *in situ* measurements. Knowing the sediment thermal properties, the depth estimation range can be also defined to establish an optimal vertical distribution of temperature sensors. In contrast, the convective heat-transfer coefficient at the sediment–pipe–soil boundary, which can be assumed to be constant, could be established using information of the sewer system. In summary, understanding heat-transfer processes in sewers, coupled with the measurement of thermal dynamics, will effectively monitor sediment build-up.

ACKNOWLEDGEMENTS

The authors are indebted to the User Group of the project *CoUDlabs_TA_USFD_02_ANNULAR_Regueiro. Time series analysis of sewer temperatures in an annular flume to estimate sediment accumulation* for their support in the experimental campaign. The User Group was composed of Manuel Regueiro-Picallo, Jeroen Langeveld, María Viklander, Mehwish Taneez, Petra van Daal-Rombouts and Jessica Thorsell.

FUNDING

The experimental campaign was funded by the EU under the Horizon 2020 INFRAIA program (Co-UDlabs project. GA No. 101008626). The work developed by Manuel Regueiro-Picallo was funded within the postdoctoral fellowship programme from the Xunta de Galicia (Consellería de Cultura, Educación e Universidade, ED481B-2021-082).

Downloaded from http://iwaponline.com/wst/article-pdf/doi/10.2166/wst.2024.193/1436204/wst089113133.pdf
by guest

DATA AVAILABILITY STATEMENT

The data collected in the laboratory-scale experimental campaign is openly accessible in ZENODO and available in these in-text data citation reference: Regueiro-Picallo *et al.* (2024b), with a license Creative Commons Attribution 4.0 International (CC BY-NC 4.0). https://doi.org/10.5281/zenodo.10821837.

CONFLICT OF INTEREST

There are no conflicts of interest to declare.

REFERENCES

Abdel-Aal, M., Tait, S., Mohamed, M. & Schellart, A. 2021 Using long term simulations to understand heat transfer processes during steady flow conditions in combined sewers. *Water* **13** (4), 570. doi:10.3390/w13040570.

Abu-Hamdeh, N. H. 2003 Thermal properties of soils as affected by density and water content. *Biosystems Engineering* **86** (1), 97–102. doi:10.1016/S1537-5110(03)00112-0.

Bertrand-Krajewski, J. L., Clemens-Meyer, F. & Lepot, M. 2021 *Metrology in Urban Drainage and Stormwater Management: Plug and Pray*. IWA Publishing, London, UK. doi:10.2166/9781789060119_xiii.

Blumensaat, F., Bloem, S., Ebi, C., Disch, A., Förster, C., Rodríguez, M., Maurer, M. & Rieckermann, J. 2023 The UWO dataset-long-term data from a real-life field laboratory to better understand urban hydrology at small spatiotemporal scales. *Engrxiv*. preprint. doi:10.31224/3208.

Booij, R. 1994 *Measurements of the Flow Field in A Rotating Annular Flume. Communications on Hydraulic and Geotechnical Engineering*, Rep. no 94-2, Delft University of Technology, Delft, The Netherlands.

Cecchetto, M. 2017 *The Development of Stochastic Based Transport Models to Predict the Advection and Diffusion of Bed-Load Sediment*. PhD Thesis, University of Sheffield, Sheffield, UK.

DeWeese, T., Tonina, D. & Luce, C. 2017 Monitoring streambed scour/deposition under nonideal temperature signal and flood conditions. *Water Resources Research* **53** (12), 10257–10273. doi:10.1002/2017WR020632.

Dürrenmatt, D. J., Del Giudice, D. & Rieckermann, J. 2013 Dynamic time warping improves sewer flow monitoring. *Water Research* **47** (11), 3803–3816. doi:10.1016/j.watres.2013.03.051.

Figueroa, A., Hadengue, B., Leitão, J. P., Rieckermann, J. & Blumensaat, F. 2021 A distributed heat transfer model for thermal-hydraulic analyses in sewer networks. *Water Research* **204**, 117649. doi:10.1016/j.watres.2021.117649.

He, H., Dyck, M. F., Horton, R., Ren, T., Bristow, K. L., Lv, J. & Si, B. 2018 Development and application of the heat pulse method for soil physical measurements. *Reviews of Geophysics* **56** (4), 567–620. doi:10.1029/2017RG000584.

Hewitt, G. F., Shires, G. L. & Bott, T. R. 1994 *Process Heat Transfer*. CRC Press, Boca Raton, FL, USA.

Lange, R. L. & Wichern, M. 2013 Sedimentation dynamics in combined sewer systems. *Water Science and Technology* **68** (4), 756–762. doi:10.2166/wst.2013.278.

Lepot, M., Pouzol, T., Aldea Borruel, X., Suner, D. & Bertrand-Krajewski, J. L. 2017 Measurement of sewer sediments with acoustic technology: From laboratory to field experiments. *Urban Water Journal* **14** (4), 369–377. doi:10.1080/1573062X.2016.1148181.

Luce, C. H., Tonina, D., Gariglio, F. & Applebee, R. 2013 Solutions for the diurnally forced advection-diffusion equation to estimate bulk fluid velocity and diffusivity in streambeds from temperature time series. *Water Resources Research* **49** (1), 488–506. doi:10.1029/2012WR012380.

Marín, E., Pichardo, J. L., Cruz-Orea, A., Diaz, P., Torres-Delgado, G., Delgadillo, I., Alvarado-Gil, J. J., Mendoza-Alvarez, J. G. & Vargas, H. 1996 On the thermal characterization of two-layer systems by means of the photoacoustic effect. *Journal of Physics D: Applied Physics* **29** (4), 981. doi:10.1088/0022-3727/29/4/006.

Montserrat, A., Bosch, L., Kiser, M. A., Poch, M. & Corominas, L. 2015 Using data from monitoring combined sewer overflows to assess, improve, and maintain combined sewer systems. *Science of the Total Environment* **505**, 1053–1061. doi:10.1016/j.scitotenv.2014.10.087.

Nikiforova, T., Savytskyi, M., Limam, K., Bosschaerts, W. & Belarbi, R. 2013 Methods and results of experimental researches of thermal conductivity of soils. *Energy Procedia* **42**, 775–783. doi:10.1016/j.egypro.2013.12.034.

Panasiuk, O., Hedström, A., Langeveld, J., de Haan, C., Liefting, E., Schilperoort, R. & Viklander, M. 2019 Using distributed temperature sensing (DTS) for locating and characterising infiltration and inflow into foul sewers before, during and after snowmelt period. *Water* **11** (8), 1529. doi:10.3390/w11081529.

Plihal, H., Kretschmer, F., Schwarz, D. & Ertl, T. 2014 Innovative sewer inspection as a basis for an optimised condition-based maintenance strategy. *Water Practice and Technology* **9** (1), 88–94. doi:10.2166/wpt.2014.010.

Radhakrishnan, A., Lu, Z. & Kandlikar, S. G. 2010 Effective thermal conductivity of gas diffusion layers used in PEMFC: Measured with guarded-hot-plate method and predicted by a fractal model. *ECS Transactions* **33** (1), 1163. doi:10.1149/1.3484610.

Ravazzani, G. 2017 Open hardware portable dual-probe heat-pulse sensor for measuring soil thermal properties and water content. *Computers and Electronics in Agriculture* **133**, 9–14. doi:10.1016/j.compag.2016.12.012.

Regueiro-Picallo, M., Naves, J., Anta, J., Suárez, J. & Puertas, J. 2017 Monitoring accumulation sediment characteristics in full scale sewer physical model with urban wastewater. *Water Science and Technology* **76** (1), 115–123. doi:10.2166/wst.2017.118.

Downloaded from http://iwaponline.com/wst/article-pdf/doi/10.2166/wst.2024.193/1436204/wst089113133.pdf
by guest

Regueiro-Picallo, M., Suárez, J., Sañudo, E., Puertas, J. & Anta, J. 2020 New insights to study the accumulation and erosion processes of fine-grained organic sediments in combined sewer systems from a laboratory scale model. *Science of the Total Environment* **716**, 136923. doi:10.1016/j.scitotenv.2020.136923.

Regueiro-Picallo, M., Anta, J., Naves, A., Figueroa, A. & Rieckermann, J. 2023 Towards urban drainage sediment accumulation monitoring using temperature sensors. *Environmental Science: Water Research & Technology* **9**, 3200–3212. doi:10.1039/D2EW00820C.

Regueiro-Picallo, M., Langeveld, J., Wei, H., Bertrand-Krajewski, J. L. & Rieckermann, J. 2024a Combining a daily temperature pattern analysis and a heat-pulse system to estimate sediment depths in sewer systems. *Environmental Science: Water Research & Technology* **10**, 922–935. doi:10.1039/D3EW00825H.

Regueiro-Picallo, M., Schellart, A., Jensen, H., Tait, S. & Fung, W. W. V. 2024b Time series analysis of sewer temperatures in an annular flume to estimate sediment accumulation. *Zenodo*. doi:10.5281/zenodo.10821838.

Ristenpart, E. 1995 Sediment properties and their changes in a sewer. *Water Science and Technology* **31** (7), 77–83. doi:10.1016/0273-1223(95)00325-H.

Sebok, E., Engesgaard, P. & Duque, C. 2017 Long-term monitoring of streambed sedimentation and scour in a dynamic stream based on streambed temperature time series. *Environmental Monitoring and Assessment* **189**, 1–15. doi:10.1007/s10661-017-6194-x.

Tait, S. J., Ashley, R. M., Verhoeven, R., Clemens, F. H. L. R. & Aanen, L. 2003 Sewer sediment transport studies using an environmentally controlled annular flume. *Water Science and Technology* **47** (4), 51–60. doi:10.2166/wst.2003.0219.

Tonina, D., Luce, C. & Gariglio, F. 2014 Quantifying streambed deposition and scour from stream and hyporheic water temperature time series. *Water Resources Research* **50** (1), 287–292. doi:10.1002/2013WR014567.

Vosse, M., Schilperoort, R., de Haan, C., Nienhuis, J., Tirion, M. & Langeveld, J. 2013 Processing of DTS monitoring results: Automated detection of illicit connections. *Water Practice and Technology* **8** (3–4), 375–381. doi:10.2166/wpt.2013.037.

First received 29 May 2024; accepted in revised form 30 May 2024. Available online 3 June 2024

Downloaded from http://iwaponline.com/wst/article-pdf/doi/10.2166/wst.2024.193/1436204/wst089113133.pdf
by guest